

promoting access to White Rose research papers



Universities of Leeds, Sheffield and York
<http://eprints.whiterose.ac.uk/>

This is an author produced version of a paper published in **Astrophysical Journal Letters**.

White Rose Research Online URL for this paper:
<http://eprints.whiterose.ac.uk/9259>

Published paper

Howe, R., Christensen-Dalsgaard, J., Hill, F., Komm, R., Schou, R., Thompson, M.J. (2009) *A note on the torsional oscillation at solar minimum*, *Astrophysical Journal Letters*, 701 (2), pp. L87-L90

<http://dx.doi.org/10.1088/0004-637X/701/2/L87>

A NOTE ON THE TORSIONAL OSCILLATION AT SOLAR MINIMUM

R. Howe,¹

rho@noao.edu

J. Christensen-Dalsgaard,² F. Hill,¹ R. Komm¹, J. Schou,³ and M. J. Thompson⁴

ABSTRACT

We examine the evolution of the zonal flow pattern in the upper solar convection zone during the current extended solar minimum, and compare it with that during the previous minimum. The results suggest that a configuration matching that at the previous minimum was reached during 2008, but that the flow band corresponding to the new cycle has been moving more slowly towards the equator than was observed in the previous cycle, resulting in a gradual increase in the apparent length of the cycle during the 2007–2008 period. The current position of the lower-latitude fast-rotating belt corresponds to that seen around the onset of activity in the previous cycle.

Subject headings: Sun: activity, Sun: helioseismology, Sun: rotation

1. INTRODUCTION

The onset of Solar Cycle 24 appears to be later than expected; nearly thirteen years after the Cycle 23 minimum in mid-1996 there is still very little surface magnetic activity. In this Letter we examine the large-scale zonal flow pattern seen in the upper convection zone in recent observations and compare the results with those for the previous solar minimum.

The migrating zonal flow pattern known as the torsional oscillation was first detected by Howard & Labonte (1980) in Doppler measurements at the solar surface carried out at the Mount Wilson Observatory; it consists of belts of slightly faster than average rotation that migrate from mid-latitudes to the equator and poles. The migration of the zonal flow bands during the solar

¹National Solar Observatory, P.O. Box 26732, Tucson AZ 85726-6732, USA

²Department of Physics and Astronomy, Aarhus University, DK-8000 Aarhus C, Denmark

³HEPL Solar Physics, 452 Lomita Mall, Stanford University, Stanford, CA 94305-4085, USA

⁴School of Mathematics and Statistics, University of Sheffield, Hounsfield Road, Sheffield S3 7RH, UK

cycle is closely connected to the migration of the magnetic activity belt. The flow pattern was first detected helioseismically by Kosovichev & Schou (1997) in early f -mode data from the Michelson Doppler Imager (MDI) aboard the Solar and Heliospheric Observatory spacecraft, and was seen to migrate by Schou (1999). Using p -mode data it is possible to resolve the depth penetration of the flows; however, only the North–South symmetric part of the pattern can be detected using global-mode helioseismology. The first four/five years of zonal-flow results from Global Oscillation Network Group (GONG) and MDI p -mode and f -mode data were reported by Howe et al. (2000), while Antia & Basu (2001) and Schou (2003) drew attention to the high-latitude part of the pattern. The further evolution of the pattern in Cycle 23 was described by Vorontsov et al. (2002); Basu & Antia (2003); Howe et al. (2005), and by Howe et al. (2006), who also considered the updated Doppler observations from Mount Wilson. The analysis of Antia et al. (2008) extends these investigations into the current solar minimum. It became evident that the torsional oscillation pattern penetrates through a significant fraction of the convection zone; Howe et al. (2005) also found some phase variation with depth in the lower-latitude, equatorward-moving part of the pattern, in the sense that the increase in rotation rate happens at earlier times at deeper depths. The lower-latitude branch of the pattern migrates equatorward with the activity belts, starting at about 45 deg latitude a few years before the previous solar minimum and reaching the equator a couple of years after maximum; the broader, stronger belt poleward of 45 deg propagates poleward on a rather shorter timescale. The whole phenomenon is usually believed to be a side-effect of the dynamo that drives the solar cycle, either directly through the Lorentz effect (Schuessler 1981) or indirectly through geostrophic effects in the activity belt (Spruit 2003). Nevertheless, the bands are clearly detectable even when there are few or no organized active regions, as was seen in the early years of Cycle 23 and again at the dawn of Cycle 24. The magnetic or sunspot butterfly diagram does not exhibit purely periodic behavior; similarly, there is no reason to expect that the zonal flow pattern should repeat precisely from cycle to cycle, but it is interesting to compare the flows seen at different minima and the way they evolve.

In this Letter, we consider the behavior of the flows around the current and previous solar minima. We concentrate on the equatorward-moving part, basing our comparisons on latitudes equatorwards of 45 deg, and on the upper part of the convection zone where the signal is clearest.

2. DATA

We now have inferences of the solar interior rotation rate, $\Omega(r, \theta)$ where r is radius and θ is latitude, covering the period from mid-1995 (GONG) and mid-1996 (MDI) to early 2009. These inferences were obtained using 2-dimensional regularized least-squares inversions on sets of medium-degree p -mode data from a total of 137 GONG time series (108 days, with start times

at 36-day intervals) and 64 non-overlapping MDI time series of 72 days each, contiguous except for the interruptions due to SOHO problems in 1998 and 1999. Details of the data analysis and inversion techniques are given in Howe et al. (2005) and references therein. The inversions are carried out on a mesh with 48 equal intervals in latitude and 50 non-uniform intervals in radius; the radial mesh was chosen to be approximately uniform in acoustical radius. To reveal the torsional oscillation signal, at each location a temporal mean over all epochs was subtracted from the rotation-rate inference. The mean was calculated separately for MDI and GONG inversions, before the residuals were combined into one time series.

The synoptic magnetic index used here has been derived from a combination of KPVT¹ and SOLIS VSM² magnetograms.

3. RESULTS AND ANALYSIS

Figure 1 shows the zonal flow pattern as a function of latitude and time at $0.99R_{\odot}$. The most recent MDI observations processed are from early 2009. Overlaid are contours of the gross magnetic longitudinal magnetic field strength. The branch of the torsional oscillation pattern corresponding to Cycle 24 is well established and clearly visible, but is moving more slowly towards the equator than did the corresponding branch in Cycle 23. The low-latitude near-surface flow profile in this data set is best matched by that at date 1997.3, as shown by the left-hand vertical line in the figure. At this point in cycle 23, substantial magnetic activity was just starting, as illustrated by the latitudinal magnetic profiles in Figure 2. The level of activity seen for the current cycle is much lower, but what hints of new-cycle activity there are seem to be at the correct latitude. Note also that there seem to have still been a few old-cycle active regions around at this point in early 1997; at present only a few very weak old-cycle regions are seen, for example, NOAA 11016 on 2009 April 29 — May 1. To give an idea of the depth dependence of the flows, Figure 1 also shows twelve-month averages of the residuals in the r, θ plane for four selected low-activity epochs. The radial detail of these profiles should not be over-interpreted, due to the poorer signal-to-noise ratio of the inversions in the interior and the varying resolution of different inversions, but the penetration of the flow belt into the bulk of the convection zone is clear.

How does the evolution of the flows during the current minimum correspond to what was seen in the previous one? To quantify this, we consider the linear correlation between the near-surface residuals $\delta\Omega(\theta, r, t_1)$ at each time step t_1 and those at a reference epoch t_0 , $\delta\Omega(\theta, r, t_0)$.

¹Available from <http://nsokp.nso.edu/dataarch.html>

²Available from <http://solis.nso.edu>

The correlation coefficient between two variables $x(t_0)$ and $x(t_1)$ is defined (Bevington 1969) as

$$C(t_0, t_1) = \frac{\sum_i [x_i(t_0) - \bar{x}(t_0)][x_i(t_1) - \bar{x}(t_1)]}{\{\sum_i [x_i(t_0) - \bar{x}(t_0)]^2\}^{1/2} \{\sum_i [x_i(t_1) - \bar{x}(t_1)]^2\}^{1/2}}, \quad (1)$$

where in this case $x_i(t) \equiv \delta\Omega(\mathbf{r}_i, t)$ and the index i enumerates inversion mesh points \mathbf{r}_i with radius $0.97 \leq r/R_\odot \leq 0.995$ and $0 \leq \theta \leq 45$ deg. In Figure 3 we show the results of this analysis for four selected reference epochs. For a reference epoch of 1995.5 (Figure 3a), about a year before the last solar minimum, the correlation reaches a maximum value around the second half of 2006 to early 2007 and then declines sharply. When the reference epoch is at 1996.5, corresponding to the previous solar minimum, (Figure 3b) the correlation coefficient reaches a maximum around the middle of 2008, and then starts to decline. A reference epoch of 2006.5 (Figure 3c) gives a maximum correlation at the beginning of the observations, 1995.5, while a reference epoch of the most recent set of observations, 2009.2, gives a correlation peaking at 1997.3, about eleven months after solar minimum (Figure 3d).

To study the temporal evolution of the apparent cycle length, for each data set from the beginning of 2007 onwards we evaluate equation (1) over latitudinal mesh points up to 45 deg, but separately at each radial mesh point from 0.973 to 0.995 R_\odot , and find the date of the highest correlation value in the early part of the cycle. The difference between this date and the reference epoch gives an estimate of cycle length in years; we then take the mean and standard deviation of these lengths at each time step, thus obtaining an estimate of the effective cycle length and its uncertainty as a function of time. The results, seen in Figure 4, seem to suggest that the effective length of the cycle measured in this manner has been slowly increasing through 2007–2008.

An alternative approach to describing the temporal variation of the flows, introduced by Vorontsov et al. (2002), is to fit the variation at each location with a sinusoid function. Howe et al. (2005) showed that, for the data through 2004, the variation was well described by fitting with an 11-year period sine wave and its second harmonic, but did not find it practical to investigate other possible cycle lengths with only nine years of observations. With nearly fourteen years of data, we can now test the fit with other cycle lengths. The time variation of the rotation at each location is modeled as

$$\Omega(r, \theta, t) = \Omega_0(r, \theta) + A_1 \sin(2\pi t/P) + A_2 \cos(2\pi t/P) + A_3 \sin(4\pi t/P) + A_4 \cos(4\pi t/P), \quad (2)$$

where P is the period in years and time t is also measured in years. We then vary P over the range from 9 to 14 years and find the value which gives the lowest χ^2 at each mesh point, before taking the mean result and its standard deviation over the range $0.97 \leq r/R_\odot \leq 0.995$. Again, we see a tendency to gradually increasing perceived cycle length in these best-fit periods, as shown by the curve in Figure 4. Taking these two analyses together, we estimate that the length of the cycle in the region equatorwards of 45 deg increased from about 11.2 to 12.2 years between early 2007

and early 2009. We have carried out a similar sine-wave analysis at higher latitudes; poleward of 60 deg the cycle length remains almost constant at about 12 years over the same period, while at intermediate latitudes the behavior is more complicated and not clearly periodic. In other words, the flow configuration, in agreement with other indicators, seems to indicate a prolonged minimum, with the flow belts (and, presumably, the almost-undetectable magnetic activity belts) moving more slowly towards the equator than was the case during the previous minimum.

4. CONCLUSION

The zonal flow pattern during the current solar minimum, considered alongside that for the previous minimum and the magnetic butterfly diagram, suggests that the minimum was reached during 2008, giving a length of approximately 12 years for Cycle 23. The flow band associated with the new cycle has been moving more slowly towards the equator than that observed during the previous minimum.

It would not be surprising to see a rapid increase in activity in the near future; it is tempting to suggest that if the current low levels persist for much longer we may indeed be looking at an unusually weak cycle.

In follow-up work, we will investigate the behavior of the flows in more detail, including the poleward branch and the flow in the deeper layers.

This work utilizes data obtained by the Global Oscillation Network Group (GONG) program, managed by the National Solar Observatory, which is operated by AURA, Inc. under a cooperative agreement with the National Science Foundation. The data were acquired by instruments operated by the Big Bear Solar Observatory, High Altitude Observatory, Learmonth Solar Observatory, Udaipur Solar Observatory, Instituto de Astrofísica de Canarias, and Cerro Tololo Interamerican Observatory. The Solar Oscillations Investigation (SOI) involving MDI is supported by NASA grant NAG 5-13261 to Stanford University. *SOHO* is a mission of international cooperation between ESA and NASA. RK, and RH in part, were supported by NASA contracts S-92698-F, NAG 5-11703, and NNG 05HL41I. NSO/Kitt Peak data used here were produced cooperatively by NSF/NOAO, NASA/GSFC, and NOAA/SEL; SOLIS data are produced cooperatively by NSF/NSO and NASA/LWS.

REFERENCES

Antia, H. M., & Basu, S. 2001, *ApJ*, 559, L67

- Antia, H. M., Basu, S., & Chitre, S. M. 2008, *ApJ*, 681, 680
- Basu, S., & Antia, H. M. 2003, *ApJ*, 585, 553
- Bevington, P. R. 1969, *Data Reduction and Error Analysis for the Physical Sciences*, McGraw Hill, New York
- Howard, R., & Labonte, B. J. 1980, *ApJ*, 239, L33
- Howe, R., Christensen-Dalsgaard, J., Hill, F., Komm, R., Schou, J., & Thompson, M. J. 2005, *ApJ*, 634, 1405
- Howe, R., Christensen-Dalsgaard, J., Hill, F., Komm, R. W., Larsen, R. M., Schou, J., Thompson, M. J., & Toomre, J. 2000, *ApJ*, 533, L163
- Howe, R., Komm, R., Hill, F., Ulrich, R., Haber, D. A., Hindman, B. W., Schou, J., & Thompson, M. J. 2006, *Sol. Phys.*, 235, 1
- Kosovichev, A. G., & Schou, J. 1997, *ApJ*, 482, L207
- Schou, J. 1999, *ApJ*, 523, L181
- Schou, J. 2003, In *Stellar astrophysical fluid dynamics*. Edited by Michael J. Thompson, Jørgen Christensen-Dalsgaard. Cambridge (UK): Cambridge University Press, ISBN 0-521-81809-5, p. 247-262
- Schuessler, M. 1981, *A&A*, 94, L17
- Spruit, H. C. 2003, *Sol. Phys.*, 213, 1
- Vorontsov, S. V., Christensen-Dalsgaard, J., Schou, J., Strakhov, V. N., & Thompson, M. J. 2002, *Science*, 296, 101

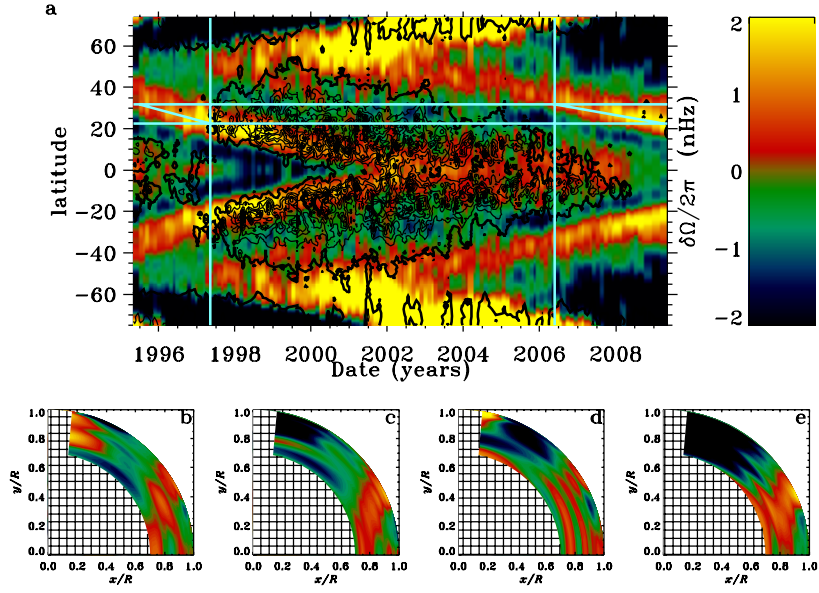


Fig. 1.— (a) Rotation-rate residuals at $0.99R_{\odot}$ from MDI and GONG. Overlaid contours show the gross longitudinal magnetic field strength from KPVT/SOLIS, at 5G intervals. The leftmost solid vertical light-blue line shows the date, 1997.3, at which the low-latitude flow configuration best matches that in the most recent (2009.2) data set, and rightmost vertical line the date, 2006.4, where it best matches that in the earliest data set (1996.5), while the horizontal lines show the respective location of the flow bands and the slanted lines schematically indicate the migration of the equatorward branch. The lower panels show 12-month averages of the rotation-rate residuals in the r, θ plane for epochs starting at (b) 1995.5, (c) 1996.3, (d) 2006.5, (e) 2008.2.

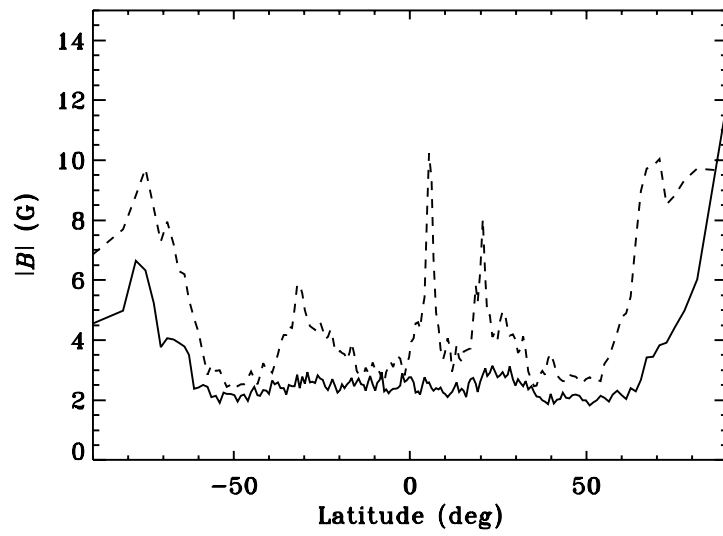


Fig. 2.— KPVT/SOLIS gross longitudinal magnetic field strength as a function of latitude, for the 2009.2 epoch of the most recent zonal flow observations (solid line) and for the epoch, 1997.3, during the previous minimum where the flows most closely match the most recent ones (dashed line).

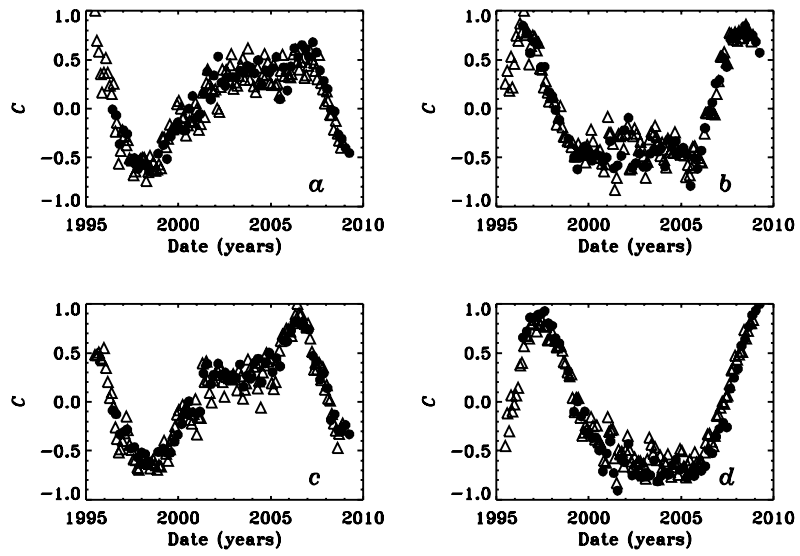


Fig. 3.— Correlation between near-surface rotation residuals at each time sample and those at selected reference epochs. Triangles represent GONG data and circles MDI. The reference epochs are: (*a*) one of the earliest sets of GONG observations at 1995.5; (*b*) the solar minimum at 1996.5; (*c*) the epoch 2006.5, chosen to give the best match to the earliest observations; and (*d*) the last set of observations we have at 2009.2.

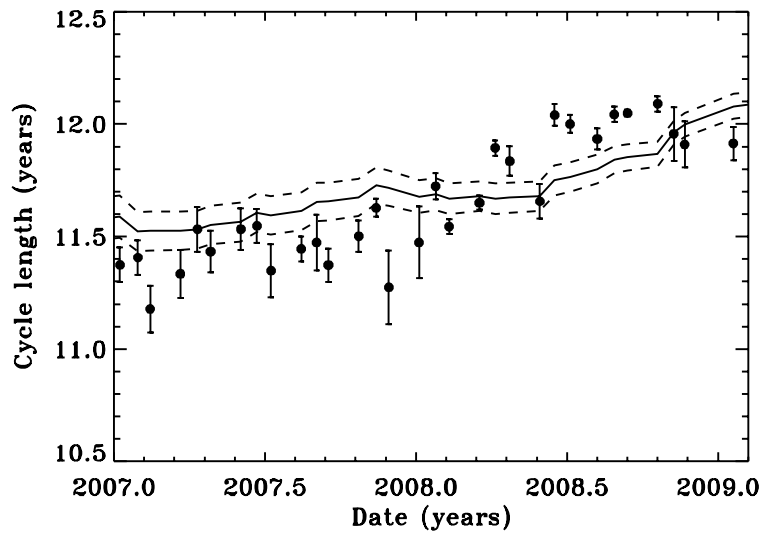


Fig. 4.— Estimated length of cycle as a function of last observing time, averaged over $0.97 \leq r/R_{\odot} \leq 0.995$ and latitude less than 45 deg. Results are derived from time lag for best correlation (symbols, with the error bar representing the standard deviation of the mean), and length of cycle estimated by sinusoid fit (solid line, with standard deviation of the mean shown by the dotted lines).